

Variable Acceleration Force Calibration System (VACS)

Ray D. Rhew¹ and Dr. Peter A. Parker¹
NASA Langley Research Center

Dr. Thomas H. Johnson²
Institute for Defense Analysis (IDA)

and

Dr. Drew Landman³
Old Dominion University

Conventionally, force balances have been calibrated manually, using a complex system of free hanging precision weights, bell cranks, and/or other mechanical components. Conventional methods may provide sufficient accuracy in some instances, but are often quite complex and labor-intensive, requiring three to four man-weeks to complete each full calibration. To ensure accuracy, gravity-based loading is typically utilized. However, this often causes difficulty when applying loads in three simultaneous, orthogonal axes. A complex system of levers, cranks, and cables must be used, introducing increased sources of systematic error, and significantly increasing the time and labor intensity required to complete the calibration. Automated machines are also used to improve calibration time however they too requires complex systems.

One aspect of the VACS is a method wherein the mass utilized for calibration is held constant, and the acceleration is changed to thereby generate relatively large forces with relatively small test masses. Multiple forces can be applied to a force balance without changing the test mass, and dynamic forces can be applied by rotation or oscillating acceleration. If rotational motion is utilized, a mass is rigidly attached to a force balance, and the mass is exposed to a rotational field. A large force can be applied by utilizing a large rotational velocity. A centrifuge or rotating table can be used to create the rotational field, and fixtures can be utilized to position the force balance. The acceleration may also be linear. For example, a table that moves linearly and accelerates in a sinusoidal manner may also be utilized. The test mass does not have to move in a path that is parallel to the ground, and no re-leveling is therefore required. Balance deflection corrections may be applied passively by monitoring the orientation of the force balance with a three-axis accelerometer package. Deflections are measured during each test run, and adjustments with respect to the true applied load can be made during the post-processing stage.

This paper will present the development and testing of the VASC concept.

Nomenclature

| | | |
|-----------|---|-----------------------|
| <i>AF</i> | = | Axial Force |
| <i>B</i> | = | balance moment center |
| <i>D</i> | = | moment distance |

¹ Research Engineer, NASA Langley Research Center, Hampton, Virginia, 23681, USA.

² Insert Job Title, Institute for Defense Analysis, Alexandria, Virginia, 22311, USA.

³ Professor, Old Dominion University, Norfolk, Virginia, 23529, USA.

| | | |
|------------|---|----------------------|
| <i>lbs</i> | = | pounds |
| <i>NF</i> | = | Normal Force |
| <i>PM</i> | = | Pitching Moment |
| <i>R</i> | = | arm length |
| <i>SVS</i> | = | Single Vector System |
| T_x | = | translational offset |
| θ | = | balance pitch angle |
| ω | = | angular velocity |

I. Background

The three most common calibration systems of today include manual dead weight calibration stands, automated pneumatic calibration machines and the single vector system (SVS). To begin, a background on these three systems is provided in context with their operational complexity and associated cost.

Manual dead weight calibration stands (figure 1) are considered the standard method of calibration since the 1940's. This type of system produces accurate results, but it suffers from operational complexity. Gravity based loads are applied via a complex system of levers, bell-cranks, cables, knife-edges, moment arms and optical alignment devices. Multiple orthogonal cables are used to apply individual components of loads. After each load is applied, the balance is re-leveled prior to taking data to assure that the applied loads are orthogonal to the balance coordinate system. This system typically applies 729 different loading configurations to calculate the calibration mathematical coefficients. Manual test stand systems perform calibrations considerably slower than both the automated system and single vector system. The cost of manual test stands significantly surpasses the single vector system but is less than automated systems.



Figure 1. Manual Dead Weight Calibration Stand

Automated calibration systems, see an example in figure 2, are similar to manual test stands in that they both use multiple orthogonal force vectors to apply loads on the transducer. The main difference between these two systems is that manual test stands apply loads via hanging dead weights, while automated systems apply loads via pneumatic actuators. A sequence of pneumatically applied loads can be programmed for the entire calibration, hence making the system automated. Automated systems are the most complex and expensive type of calibration system. The price of this type of system can exceed one million dollars.

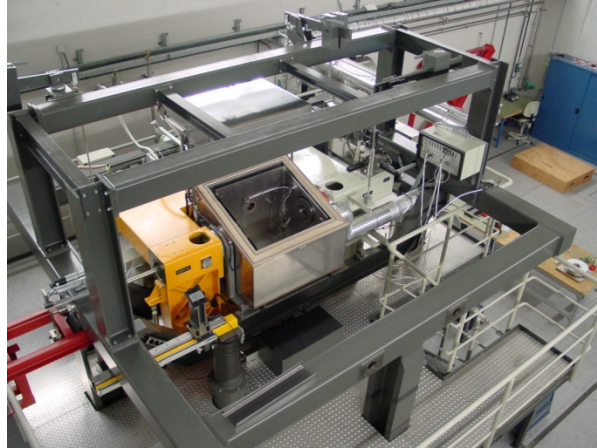


Figure 2. Automated Calibration System at the European Transonic Wind Tunnel

The current state of the art calibration system used at NASA Langley Research Center is the Single Vector System (SVS) depicted in figure 3 and discussed further in reference 1. The SVS is unique because it is the only force transducer calibration system that uses a single applied force vector, gravity. By pitching and rolling the transducer, and by changing the location of the applied gravitational force relative to the transducer moment center, combinations of all six force components can be achieved. This loading technique in conjunction with a statistically rigorous loading sequence makes the SVS the preferred method for calibration at LaRC since 2001. The statistical approach unique to the SVS is based upon three pillars: replication of calibration runs, blocking of sets of calibration runs and randomizing the order of calibration runs. Replication and randomization allows for a test of internal systemic error and provides a check for technician set point errors. Blocking helps defend against nuisance errors that are uncontrollable during the experiment. This statistical approach complements the SVS hardware by allowing for a minimal number of configurations during the calibration. The single vector system uses less hardware compared to the other calibration systems; hence it is considered the mechanically simplest of the three systems. Since there is only one applied force vector and re-leveling is not required, the SVS is nearly as fast as automated systems. The SVS is also the least expensive system, costing around \$50,000. Now that the three major calibration systems have been introduced, problems associated with dead weights are discussed.

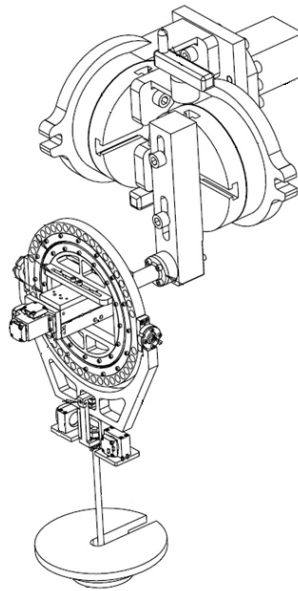


Figure 3. Single Vector System

In any industry, there is always a cost associated with moving weight. A large problem with the SVS and manual test stand is that they use dead weight to apply loads on the transducer. Between calibration runs, the weight is manually removed or added by the operator. This process can become slow and tedious when the weight has to be changed many times throughout the entire calibration experiment. For large scale transducers, upwards of 2,500 lbs can be added and then later removed. Such a large amount of weight could take up to twenty minutes to setup before data is taken. Additionally, the SVS has a structural limitation of 3,000lbs. The hardware is designed to this specification, however calibrating near this limit is considered extremely inefficient. Balances that require calibration loads greater than 3,000 lbs cannot be calibrated using the SVS.

Another problem common to manual test stands and some automated calibration systems is that they require balance repositioning after each load is applied in order to account for balance deflection and to assure that the multiple loads are applied orthogonally. There are two concerns associated with repositioning and multiple applied vectors. First, since the loads are applied sequentially, the bias error associated with the instruments used to apply a single load compounds with each additional load applied thereafter. The second major concern is that manual stands and automated systems have a parallel path to ground, meaning that both the metric and non-metric end of the transducer have boundary conditions reference to ground. In the case of the automated system, the non-metric end of the transducer is fixed, while the metric end is attached to a pneumatic actuator which is then attached to ground. Manual test stands, however, do not have a parallel path to ground when applying a normal force load. For normal force loads, the non-metric end is fixed, while the metric end is attached to a free hanging weight via a cable. For side or axial force loads, a manual test stand requires a pulley attached to ground; hence the parallel path to ground in these situations is formed. This gives rise to an iterative re-leveling procedure, which is not only time consuming, but also introduces extra degrees of freedom that further increase systematic error.

Another problem common to all three calibration systems is that they require a large footprint to operate, making them highly immobile. The inventory of weights alone for the manual stand or SVS is enough to fill a small facility. While the automated system does not require weights, it does have a bulky external frame and depends on a significant source of electricity to power the actuators. For these reasons, it is not feasible to create a mobile platform using any of these existing systems.

A final problem is that all three calibration systems are incapable of calibrating multiple balances simultaneously. A calibration facility capable of this would require multiple systems which would drastically increase cost and personnel. NASA Langley Research Center has about 400 balances in inventory. Maintaining up to date calibration information on each balance is an up-hill battle that unavoidably results in inadequate operational readiness.

II. Introduction

The key difference between the Variable Acceleration Calibration System (VACS) and other existing systems is that it uses a new force application method. VACS uses a combination of gravitational and centripetal acceleration to impart a force on a mass that is rigidly attached to the transducer. By changing the orientation of the transducer and by changing the position of the attached mass, all six components of force, as experienced by the transducer, can be achieved. There are five independent variables that are altered throughout the calibration. Angular velocity, ω , and the distance between the attached mass, m , and axis of rotation, r , are used to adjust the magnitude of applied force, F (equation 1).

$$F = mg + mr\omega^2 \tag{1}$$

The distance between the attached mass and axis of rotation is varied using a linear actuator as seen in figure 4. The transducer pitch angle and rotation angle are set using variable angle actuators as shown in figure 5. The position of the applied mass on the transducer is the fifth and final independent variable and is the only setting that cannot be changed automatically using a computer interface. There are multiple embodiments of this system that could aide in rotating the components shown in figure 4. The linear actuator assembly could be fixed to a rotating table or centrifuge. Alternatively, the linear actuator could be fastened to a rotating rod that is aligned with the axis of rotation. In either case, the axis of rotation is aligned with the gravitational vector, which is necessary to apply a steady force to the attached mass.

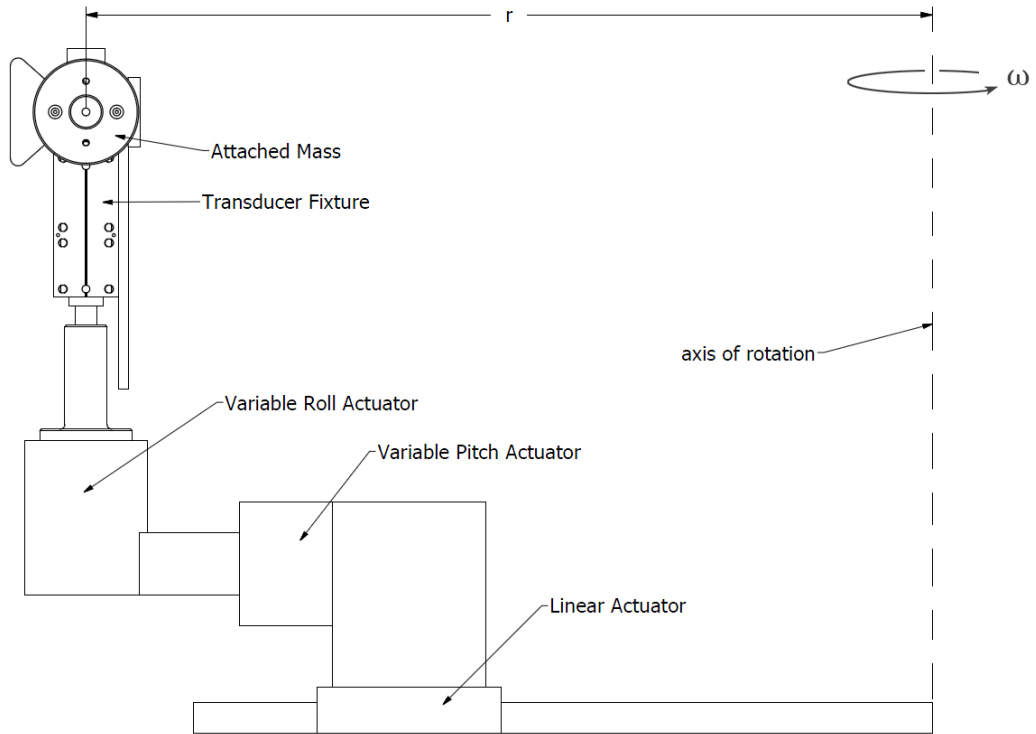


Figure 1. VACS Conceptual Layout

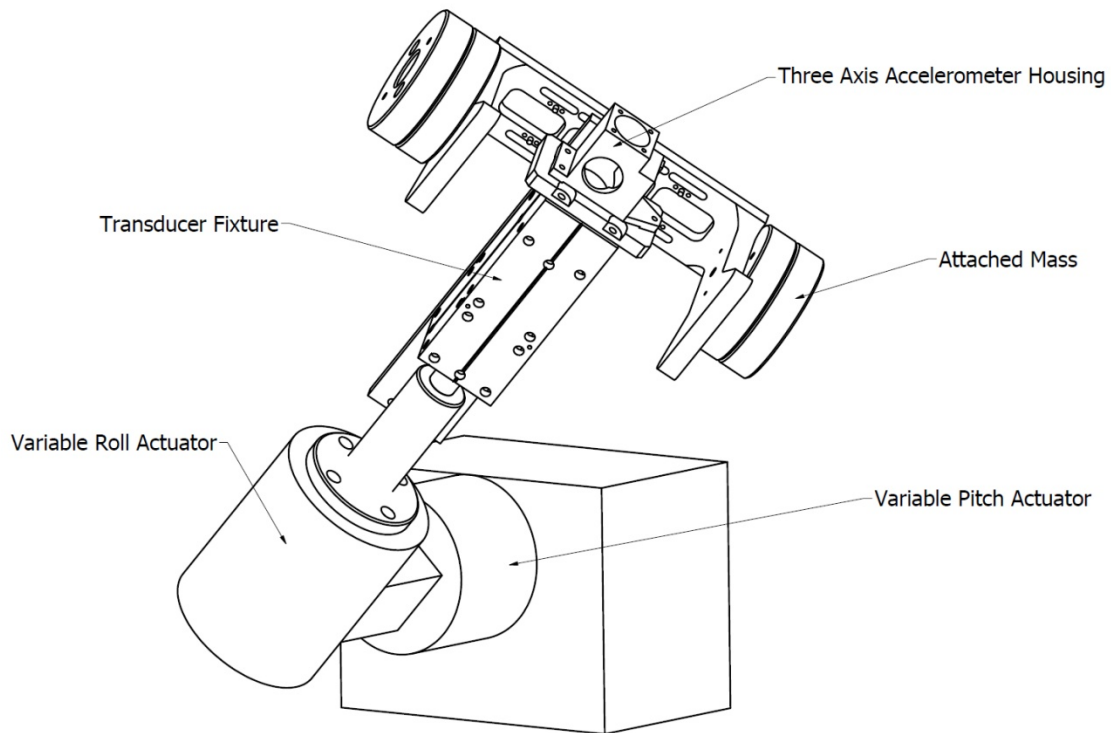


Figure 2 Variable Orientation Actuators Concept

There are several advantages to this new loading technique. The first is that there is no parallel path to ground; the non-metric end is fixed, while the metric end is free. The second advantage is that it uses a single force vector. The single force vector approach can be seen as an advantage because there is no compounded instrument bias error due to multiple applied force vectors. Additionally, there is no need to re-level the transducer to maintain orthogonality between multiple applied force vectors. The deflected transducer orientation is measured and accounted for in the experimental design using a three axis accelerometer attached at the metric end of the transducer, as seen in figure 5. The accelerometer measurements are used for deflection corrections of the true applied load in the post process stage. Roughly setting and then measuring the independent variables of the experiment provides a vast time savings as compared to iteratively attempting to precisely set all independent variables. Departures from the ideal variable settings are accounted for in the experimental design using design of experiments. Design of experiments is also used to minimize the total number of transducer configurations over the entire calibration experiment. Replication, randomization and blocking of runs are used to provide an estimate of internal systemic error, as well as to provide a check for human related error.

The most significant advantage of the VACS loading technique is that it can variably load the transducer without the need to move any weight. By increasing the angular velocity of the rotating field, the force experienced by the transducer increases. Downtime between calibration runs will be reduced because there is no need to move large amounts of weight. The same weight can be used throughout the entire calibration experiment. Furthermore, very large forces can be generated using a relatively small amount of weight using a very fast rotating field. This will allow for calibration of large scale transducers.

In conclusion, the VACS is a mechanically simple and inexpensive system as compared to manual test stands, automated systems and the SVS. The VACS is similar to the SVS because both implement design of experiments using a single vector load. The advantage of the VACS over the SVS is that there is no need to move weight. Additionally, VACS is capable of calibrating large balances that the SVS cannot. Compared to manual test stands and automated systems, VACS has fewer degrees of freedom, providing superior accuracy at a fraction of the cost.

III. Proof of Concept Development

The Variable Acceleration Calibration System (VACS) differs from existing systems because it uses both centripetal and gravitational acceleration to apply loads onto a balance. The fundamental concept uses a mass that is rigidly attached to the balance and is exposed to a constant centripetal and gravitational field. The resulting force imparted by the attached mass is shown in equation **Error! Reference source not found.**

A large force can be applied using a relatively small amount of weight and a large rotational velocity. As a result, less weight is moved during the calibration process leading to a decrease in calibration time compared to traditional dead weight loading methods.

Two proof-of-concept systems have been constructed to demonstrate the feasibility of the variable acceleration concept. The hardware of both is designed around a specific set of calibration runs that loads multiple components simultaneously. The prototypes differ in the way the balance is positioned in the rotational field, and where the mass is attached to the balance. The first prototype, referred to as the "centered system," has the balance centered on the rotating table, with the balance axial force axis parallel to the axis of rotation. The second prototype, referred to as the "off-center system," differs from the centered system since it is positioned off the center of the table with its axial force axis at an angle relative to the rotation axis.

A simple two dimensional representation of both systems is shown in figure 6, where equations (1) through (3) determine the component loads on the balance. In figure 6, point O is the center of the rotating table, which rotates with angular velocity, ω . The axial force axis of the balance, also referred to as the "balance axis" is defined by the line segment AC. Point A is where the balance attaches to the table, point B is the moment center of the balance, θ is the pitch angle of the balance, and α is the misalignment angle between the table rotation axis and the gravity vector. T_x is the translational offset between the balance attachment point and the center of the table. R is the arm length between the balance axial force axis and the center of gravity of the attached weight m , while ϕ is the pitch angle of the arm with respect to line that is perpendicular to the balance axis. For the centered system, T_x and θ are zero, while for the off-center system, R is zero. Equations (1) through (3) assume constant rotational velocity and represent the average load during one revolution.

Opposing force vector loading schemes can be achieved by attaching mass on opposite sides. These coupled opposing force vectors allow for pure moment application to the balance, if the axial force contribution is tared out. As a result, the centered system is capable of employing unique combinations of simultaneously applied loads. The centrifugal force from the mass of the balance is minimized by aligning the center of gravity of the balance with the axis of rotation of the table. This helps decrease the tare loads relative to the calibration loads.

The generic governing equations are applied to each arm of the centered system, and then summed, as depicted in figure 8 and shown in equations (4) through (7). In equations (4) through (7), NF_i corresponds to the normal force imparted by the attached weight on the i th arm. There are six arms, therefore, i varies from one to six.

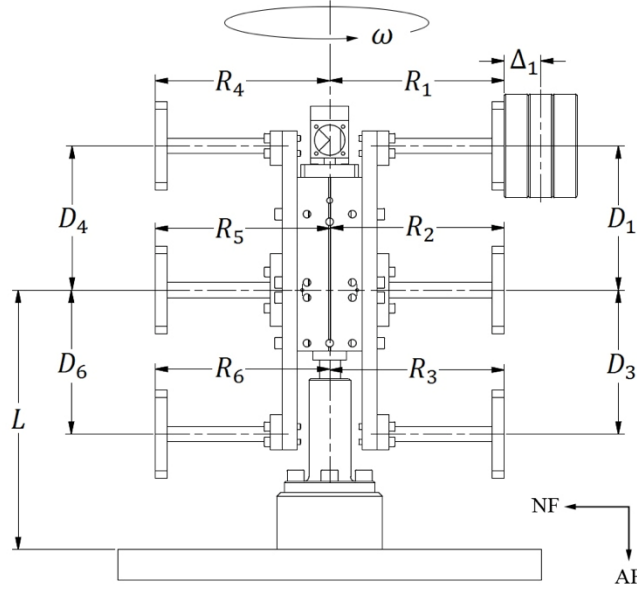


Figure 8. Centered System Modeling Example

$$NF_i = -m_i\omega^2[T_x + \sin(\theta)(L + D_i) + \cos(\phi_i)\cos(\theta)(R_i + \Delta_i) - \sin(\phi_i)\sin(\theta)(R_i + \Delta_i)]\cos(\theta) - m_i g \cos(\alpha)\sin(\theta) \quad (4)$$

$$AF_i = m_i\omega^2[T_x + \sin(\theta)(L + D_i) + \cos(\phi_i)\cos(\theta)(R_i + \Delta_i) - \sin(\phi_i)\sin(\theta)(R_i + \Delta_i)]\sin(\theta) + m_i g \cos(\alpha)\cos(\theta) \quad (5)$$

$$PM_i = [\cos(\phi_i)D_i - \sin(\phi_i)(R_i + \Delta_i)]NF_i + [\sin(\phi_i)D_i - \cos(\phi_i)(R_i + \Delta_i)]AF_i \quad (6)$$

$$NF_{Tot} = \sum_i^6 NF_i \quad AF_{Tot} = \sum_i^6 AF_i \quad PM_{Tot} = \sum_i^6 PM_i \quad (7)$$

The arm lengths, R_i , and the moment arm distances, D_i , were designed to meet the load requirements of the calibration design matrix. The parts were measured with vernier calipers, while the system was in its final assembled state. The measured arm lengths and moment arm distances, shown in **table 1**, are held constant throughout the experiment. Similarly, the distance between the balance attachment point and the balance moment center, L , is also held constant, and is equal to 8.563 inches.

Table 1. Arm Lengths for the Centered System

| Arm Length | | Moment Distance | |
|------------|-----------|-----------------|-----------|
| R_1 | 6.176 in | D_1 | 4.701 in |
| R_2 | 6.148 in | D_2 | 0.000 in |
| R_3 | 6.133 in | D_3 | -4.790 in |
| R_4 | -6.178 in | D_4 | 4.713 in |
| R_5 | -6.158 in | D_5 | 0.000 in |
| R_6 | -6.175 in | D_6 | -4.734 in |

B. Off-Centered System Concept

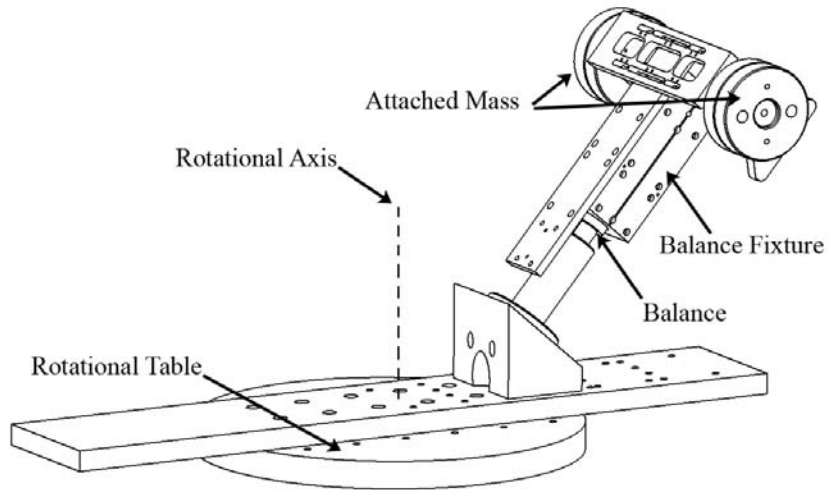


Figure 9. Off-Center System Concept

The general layout of the off-center system is shown in figure 9. Similar to the centered system, the number of independent variables for the off-center system is minimized to reduce system complexity and cost. Here, the independent variables are translation offset, pitch angle, roll angle, angular velocity and moment arm distance, as shown in figure 10. The translation offset, T_x , is changed by fastening the wedge adapter at different locations along the table adapter. The pitch angle is determined by the wedge adapter selection, while the roll angle is adjusted by detaching the balance from the wedge, and fastening at the specified roll angle. To satisfy the loading requirements of the calibration experiment, only two roll angles are required: 0 and 180 degrees. A threaded hole pattern on the fixture cover allows for the arm bracket to fasten at various locations, which effectively alters the moment arm distance, D .

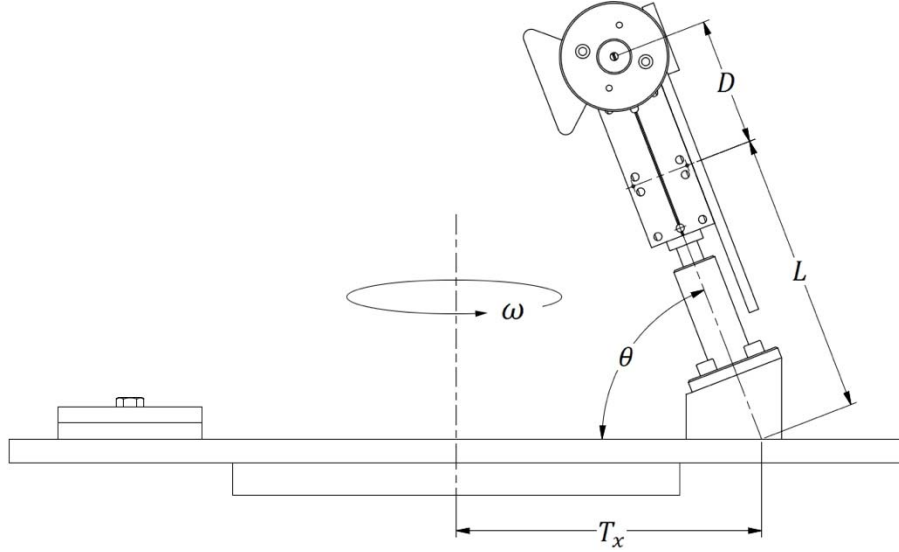


Figure 3. Off-Center System Modeling Example

For each loading configuration, the attached weight is equally spaced on either side of the arm bracket so that the center of gravity of attached weight is coincident with the axis of the balance. The arm bracket is an existing part, which is used as a force positioning system for low-weight SVS calibrations at NASA LaRC. The calibrated weights used for the centered system are similarly used here.

In contrast to the centered system, the off-center system uses a single applied force vector. As a result, the off-center system is subject to the single force vector loading constraint shown in equation (8). Details about this constraint can be found in reference 2.

$$-(RM)(AF) + (PM)(SF) - (YM)(NF) = 0 \quad (8)$$

The generic governing equations are applied to the off-center system, as shown in equations (9) through (11). In equation (9), q is equal to 1 if the balance has a zero degree roll angle (the balance is in its nominal state), while q is equal to -1 if the balance is rolled 180 degrees.

$$NF = q(-m\omega^2[T_x + \sin(\theta)(L + D) + \cos(\phi)\cos(\theta)R - \sin(\phi)\sin(\theta)R]\cos(\theta) - mg\cos(\alpha)\sin(\theta)) \quad (9)$$

$$AF = -m\omega^2[T_x + \sin(\theta)(L + D) + \cos(\phi)\cos(\theta)R - \sin(\phi)\sin(\theta)R]\sin(\theta) + mg\cos(\alpha)\cos(\theta) \quad (10)$$

$$PM = [\cos(\phi)D - \sin(\phi)R]NF + [\sin(\phi)D + \cos(\phi)R]AF \quad (11)$$

IV. Experimental Design and Set-up

The calibration experiment design accommodate the calibration model shown in equation (12).

$$R_i = a_i + \sum_{j=1}^3 \beta_{i,j}F_j + \sum_{j=1}^3 \sum_{k=j+1}^3 \beta_{i,j,k}F_jF_k \quad (12)$$

This is the standard form of a second order polynomial that is used for single-piece balance calibration models without the nonlinear or squared terms. The equation only contains 3 components since the proof of concept experiment will concentrate on normal, axial and pitch only at this time.

The balance chosen for the experiments is the UT-36 shown in figure 11. This balance was chosen due to its size and its load capacity fitting well within the size and capacity constraints of the rotational system available. Table 2 lists the balance design loads as well as the loads to be utilized for the experiment. Due to the exploratory nature of this concept, loads well under the balance capacity were chosen to ensure the balance safety was considered.



Figure 11. Off-Center System

Table 2. UT-36 Design Loads and Calibration Loads

| | NF (lbs) | AF (lbs) | PM (in-lbs) |
|----------------------|----------|----------|-------------|
| Balance Design Loads | 100 | 60 | 800 |
| Calibration Loads | 30 | 20 | 120 |

The calibration experiments, loads, for the centered and off-centered systems are shown in tables 3 and 4 respectively for the ideal case (no experimental set point error). The calibration experiments are factorial experiments in three factors. Both designs consist of eight factorial points and one center points. The design is fully replicated, which provides a total of 18 runs. Point replication is employed to provide an internal estimate of experimental error. Full replication also helps increase power, which is defined as the probability that the statistical test will reject the null hypothesis when the null hypothesis is false. Additionally employing experiment design principles, the runs a randomized to convert systematic error effects to random errors. Tables 5 and 6 show the experiment design load scheduls for each system in actual settings. The actual loads are those that were achieved during experiment execution. Table 7 reviews the effect of the actual settings on the ability to compute coefficients and shows that there is little impact with variance inflation factors near 1 (the variance inflation factor is defined in reference 3).

Document Text Table 3. Ideal Centered System Calibration Experiment

| Centered System | | | | | | | |
|-----------------|------|---------------|----------|-------------|-------------|----|----|
| Std Run# | Run# | Natural Units | | | Coded Units | | |
| | | NF (lbs) | AF (lbs) | PM (in-lbs) | NF | AF | PM |
| 1 | 4 | -30 | 6 | -120 | -1 | -1 | -1 |
| 2 | 18 | -30 | 6 | -120 | -1 | -1 | -1 |
| 3 | 9 | 30 | 6 | -120 | 1 | -1 | -1 |
| 4 | 15 | 30 | 6 | -120 | 1 | -1 | -1 |
| 5 | 2 | -30 | 20 | -120 | -1 | 1 | -1 |
| 6 | 6 | -30 | 20 | -120 | -1 | 1 | -1 |
| 7 | 5 | 30 | 20 | -120 | 1 | 1 | -1 |
| 8 | 11 | 30 | 20 | -120 | 1 | 1 | -1 |
| 9 | 10 | -30 | 6 | 120 | -1 | -1 | 1 |
| 10 | 12 | -30 | 6 | 120 | -1 | -1 | 1 |
| 11 | 17 | 30 | 6 | 120 | 1 | -1 | 1 |
| 12 | 16 | 30 | 6 | 120 | 1 | -1 | 1 |
| 13 | 1 | -30 | 20 | 120 | -1 | 1 | 1 |
| 14 | 13 | -30 | 20 | 120 | -1 | 1 | 1 |
| 15 | 14 | 30 | 20 | 120 | 1 | 1 | 1 |
| 16 | 7 | 30 | 20 | 120 | 1 | 1 | 1 |
| 17 | 8 | 0 | 13 | 0 | 0 | 0 | 0 |
| 18 | 3 | 0 | 13 | 0 | 0 | 0 | 0 |

Table 4. Ideal Off-Center System Calibration Experiment

| Off-Center System | | | | | | | |
|-------------------|------|---------------|----------|-------------|-------------|----|----|
| Std Run# | Run# | Natural Units | | | Coded Units | | |
| | | NF (lbs) | AF (lbs) | PM (in-lbs) | NF | AF | PM |
| 1 | 1 | -30 | -20 | -120 | -1 | -1 | -1 |
| 2 | 14 | -30 | -20 | -120 | -1 | -1 | -1 |
| 3 | 15 | 30 | -20 | -120 | 1 | -1 | -1 |
| 4 | 6 | 30 | -20 | -120 | 1 | -1 | -1 |
| 5 | 18 | -30 | 20 | -120 | -1 | 1 | -1 |
| 6 | 8 | -30 | 20 | -120 | -1 | 1 | -1 |
| 7 | 16 | 30 | 20 | -120 | 1 | 1 | -1 |
| 8 | 4 | 30 | 20 | -120 | 1 | 1 | -1 |
| 9 | 2 | -30 | -20 | 120 | -1 | -1 | 1 |
| 10 | 9 | -30 | -20 | 120 | -1 | -1 | 1 |
| 11 | 13 | 30 | -20 | 120 | 1 | -1 | 1 |
| 12 | 5 | 30 | -20 | 120 | 1 | -1 | 1 |
| 13 | 10 | -30 | 20 | 120 | -1 | 1 | 1 |
| 14 | 7 | -30 | 20 | 120 | -1 | 1 | 1 |
| 15 | 17 | 30 | 20 | 120 | 1 | 1 | 1 |
| 16 | 11 | 30 | 20 | 120 | 1 | 1 | 1 |
| 17 | 12 | 0 | 0 | 0 | 0 | 0 | 0 |
| 18 | 3 | 0 | 0 | 0 | 0 | 0 | 0 |

Table 5. Actual Centered System Calibration Experiment

| Centered System | | | | | | | |
|-----------------|------|---------------|----------|-------------|-------------|-------|-------|
| Std Run# | Run# | Natural Units | | | Coded Units | | |
| | | NF (lbs) | AF (lbs) | PM (in-lbs) | NF | AF | PM |
| 1 | 4 | -30.28 | 6.00 | -99.06 | -0.92 | -0.98 | -0.86 |
| 2 | 18 | -30.33 | 6.00 | -99.11 | -0.92 | -0.98 | -0.86 |
| 3 | 9 | 32.86 | 6.04 | -110.78 | 0.99 | -0.97 | -0.97 |
| 4 | 15 | 32.89 | 6.05 | -110.92 | 0.99 | -0.97 | -0.97 |
| 5 | 2 | -30.74 | 15.97 | -107.06 | -0.93 | 0.99 | -0.93 |
| 6 | 6 | -30.76 | 15.97 | -106.99 | -0.93 | 0.99 | -0.93 |
| 7 | 5 | 33.21 | 16.04 | -114.41 | 1.00 | 1.00 | -1.00 |
| 8 | 11 | 33.28 | 16.03 | -114.76 | 1.00 | 1.00 | -1.00 |
| 9 | 10 | -32.69 | 6.00 | 112.04 | -0.99 | -0.98 | 0.96 |
| 10 | 12 | -32.74 | 6.01 | 112.25 | -0.99 | -0.97 | 0.97 |
| 11 | 17 | 30.42 | 5.88 | 98.57 | 0.91 | -1.00 | 0.85 |
| 12 | 16 | 30.45 | 5.88 | 98.68 | 0.91 | -1.00 | 0.85 |
| 13 | 1 | -33.05 | 15.97 | 116.19 | -1.00 | 0.99 | 1.00 |
| 14 | 13 | -33.05 | 15.99 | 116.17 | -1.00 | 0.99 | 1.00 |
| 15 | 14 | 30.89 | 15.84 | 107.14 | 0.93 | 0.96 | 0.92 |
| 16 | 7 | 30.89 | 15.84 | 107.10 | 0.93 | 0.96 | 0.92 |
| 17 | 8 | 0.01 | 10.97 | 0.04 | 0.00 | 0.00 | -0.01 |
| 18 | 3 | 0.01 | 10.98 | 0.08 | 0.00 | 0.00 | -0.01 |

Table 6. Actual Off-Center System Calibration Experiment

| Off-Center System | | | | | | | |
|-------------------|------|---------------|----------|-------------|-------------|-------|-------|
| Std Run# | Run# | Natural Units | | | Coded Units | | |
| | | NF (lbs) | AF (lbs) | PM (in-lbs) | NF | AF | PM |
| 1 | 1 | -31.19 | -19.30 | -125.52 | -1.00 | -0.99 | -1.00 |
| 2 | 14 | -31.26 | -19.27 | -125.38 | -1.00 | -0.99 | -1.00 |
| 3 | 15 | 30.98 | -18.53 | -124.15 | 0.99 | -0.95 | -0.99 |
| 4 | 6 | 30.98 | -18.53 | -124.16 | 0.99 | -0.95 | -0.99 |
| 5 | 18 | -30.34 | 17.69 | -121.48 | -0.97 | 0.97 | -0.97 |
| 6 | 8 | -30.39 | 17.73 | -121.68 | -0.97 | 0.97 | -0.97 |
| 7 | 16 | 30.70 | 18.28 | -122.07 | 0.98 | 1.00 | -0.97 |
| 8 | 4 | 30.66 | 18.27 | -122.08 | 0.98 | 1.00 | -0.97 |
| 9 | 2 | -30.92 | -18.62 | 123.06 | -0.99 | -0.95 | 0.99 |
| 10 | 9 | -30.96 | -18.67 | 123.11 | -0.99 | -0.96 | 0.99 |
| 11 | 13 | 31.25 | -19.35 | 124.21 | 1.00 | -0.99 | 1.00 |
| 12 | 5 | 31.34 | -19.52 | 124.34 | 1.00 | -1.00 | 1.00 |
| 13 | 10 | -30.68 | 18.20 | 122.22 | -0.98 | 1.00 | 0.98 |
| 14 | 7 | -30.69 | 18.20 | 122.18 | -0.98 | 1.00 | 0.98 |
| 15 | 17 | 30.32 | 17.60 | 121.28 | 0.97 | 0.96 | 0.98 |
| 16 | 11 | 30.33 | 17.60 | 121.38 | 0.97 | 0.96 | 0.98 |
| 17 | 12 | 0.00 | 0.00 | 0.00 | 0.00 | 0.03 | 0.00 |
| 18 | 3 | 0.00 | 0.00 | 0.00 | 0.00 | 0.03 | 0.00 |

Table 7. Variance Inflation Factors for the Calibration Experiments

| Parameter | Variance Inflation Factors (VIF) | | | |
|--------------|----------------------------------|--------|-----------------|--------|
| | Off-Center System | | Centered System | |
| | Ideal | Actual | Ideal | Actual |
| β_1 | 1.000 | 1.001 | 1.000 | 1.008 |
| β_2 | 1.000 | 1.001 | 1.000 | 1.000 |
| β_3 | 1.000 | 1.001 | 1.000 | 1.011 |
| β_{12} | 1.000 | 1.001 | 1.000 | 1.008 |
| β_{13} | 1.000 | 1.001 | 1.000 | 1.000 |
| β_{23} | 1.000 | 1.001 | 1.000 | 1.011 |

The calibration loads reflect the difference between the total load and tare load. The calibration loads represent the gravitational and centrifugal force imparted by the attached weight. The tare loads represent the force imparted by the fixture and balance weights. Tare runs are performed before each run in the calibration matrix, from which tare loads are measured for a particular configuration of the calibration system. The tare loads are dynamic, meaning that a tare load is taken while the balance is spinning at the specified angular velocity, albeit with no weights attached. The centered system has the advantage that the tare loads are nearly identical for each calibration load, since the balance remains fixed in the same position throughout the calibration experiment. On the other hand, the off-center system has varying tare loads, since the balance is oriented in various off-center, asymmetric configurations throughout the calibration experiment.

Tables 8 and 9 list the independent variable settings used for each system experiment to achieve the experimental design loads. This provides some insight into how each loading is executed. Figures 12 and 13 are pictures of each experimental set-up, centered and off-center, installed on the rate table.

Table 8. Independent Variable Settings for the Centered System Experiment

| Std Run# | m_1 (lbm) | m_2 (lbm) | m_3 (lbm) | m_4 (lbm) | m_5 (lbm) | m_6 (lbm) | ω (rev/s) |
|----------|-------------|-------------|-------------|-------------|-------------|-------------|------------------|
| 1 | 2.5 | 3.5 | 0 | 0 | 0 | 0 | 2.69 |
| 2 | 2.5 | 3.5 | 0 | 0 | 0 | 0 | 2.69 |
| 3 | 0 | 0 | 0 | 0 | 0 | 6 | 2.69 |
| 4 | 0 | 0 | 0 | 0 | 0 | 6 | 2.69 |
| 5 | 3.5 | 8 | 4.5 | 0 | 0 | 0 | 1.59 |
| 6 | 3.5 | 8 | 4.5 | 0 | 0 | 0 | 1.59 |
| 7 | 3 | 0 | 0 | 0 | 3 | 10 | 1.99 |
| 8 | 3 | 0 | 0 | 0 | 3 | 10 | 1.99 |
| 9 | 0 | 0 | 6 | 0 | 0 | 0 | 2.69 |
| 10 | 0 | 0 | 6 | 0 | 0 | 0 | 2.69 |
| 11 | 0 | 0 | 0 | 2.5 | 3.5 | 0 | 2.69 |
| 12 | 0 | 0 | 0 | 2.5 | 3.5 | 0 | 2.69 |
| 13 | 0 | 3 | 10 | 3 | 0 | 0 | 1.99 |
| 14 | 0 | 3 | 10 | 3 | 0 | 0 | 1.99 |
| 15 | 0 | 0 | 0 | 3.5 | 8 | 4.5 | 1.59 |
| 16 | 0 | 0 | 0 | 3.5 | 8 | 4.5 | 1.59 |
| 17 | 5.5 | 0 | 0 | 5.5 | 0 | 0 | 0 |
| 18 | 5.5 | 0 | 0 | 5.5 | 0 | 0 | 0 |

Table 9. Independent Variable Settings for the Off-Center System

| Std Run# | m (lbm) | ω (rev/s) | L (inch) | T_x (inch) | θ_{wedge} (deg) | D (inch) | q |
|----------|-----------|------------------|------------|--------------|------------------------|------------|-----|
| 1 | 6.00 | 2.70 | 10.50 | -1.40 | 40.80 | 4.00 | 1 |
| 2 | 6.00 | 2.70 | 10.50 | -1.40 | 40.80 | 4.00 | 1 |
| 3 | 6.00 | 2.70 | 10.50 | 3.70 | 40.80 | -4.00 | -1 |
| 4 | 6.00 | 2.70 | 10.50 | 3.70 | 40.80 | -4.00 | -1 |
| 5 | 6.00 | 2.70 | 9.63 | 12.56 | -20.92 | 4.00 | 1 |
| 6 | 6.00 | 2.70 | 9.63 | 12.56 | -20.92 | 4.00 | 1 |
| 7 | 6.00 | 2.70 | 9.63 | 9.86 | -20.92 | -4.00 | -1 |
| 8 | 6.00 | 2.70 | 9.63 | 9.86 | -20.92 | -4.00 | -1 |
| 9 | 6.00 | 2.70 | 10.50 | 3.70 | 40.80 | -4.00 | 1 |
| 10 | 6.00 | 2.70 | 10.50 | 3.70 | 40.80 | -4.00 | 1 |
| 11 | 6.00 | 2.70 | 10.50 | -1.40 | 40.80 | 4.00 | -1 |
| 12 | 6.00 | 2.70 | 10.50 | -1.40 | 40.80 | 4.00 | -1 |
| 13 | 6.00 | 2.70 | 9.63 | 9.86 | -20.92 | -4.00 | 1 |
| 14 | 6.00 | 2.70 | 9.63 | 9.86 | -20.92 | -4.00 | 1 |
| 15 | 6.00 | 2.70 | 9.63 | 12.56 | -20.92 | 4.00 | -1 |
| 16 | 6.00 | 2.70 | 9.63 | 12.56 | -20.92 | 4.00 | -1 |
| 17 | 0.00 | 0.00 | 9.63 | 9.86 | -20.92 | -4.00 | -1 |
| 18 | 0.00 | 0.00 | 10.50 | 3.70 | 40.80 | -4.00 | 1 |

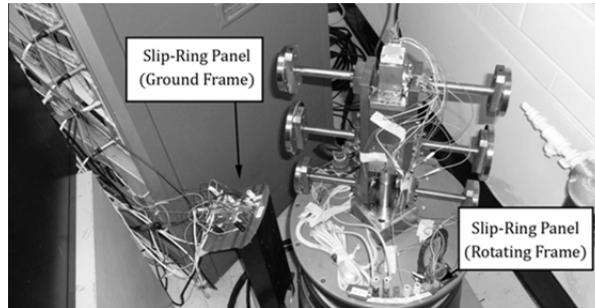


Figure 12. Centered System (with slip rings noted)

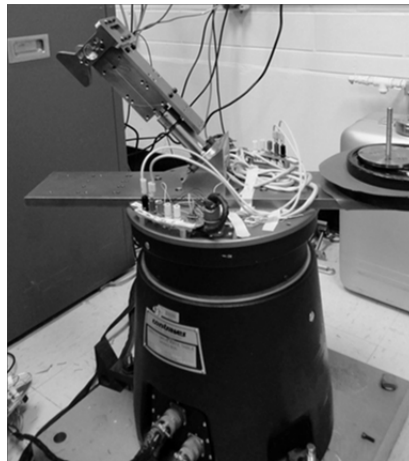


Figure 13. Off-Center System

V. Experimental Results

To evaluate the experimental results, the applied load error is presented as a percentage of the full scale loads of the calibration experiments, referred to as "percent of full scale error" (%FSE) in figures 14 and 15. The normalizing full scale loads used for each system are shown in table 10. The applied load errors were calculated as: Applied Load – Computed Load (using the previous calibration from 1995).

Table 10. Full Scales Loads used to Calculate %FSE for Both Systems

| NF (lbs) | AF (lbs) | PM (in-lbs) |
|----------|----------|-------------|
| 30 | 20 | 120 |

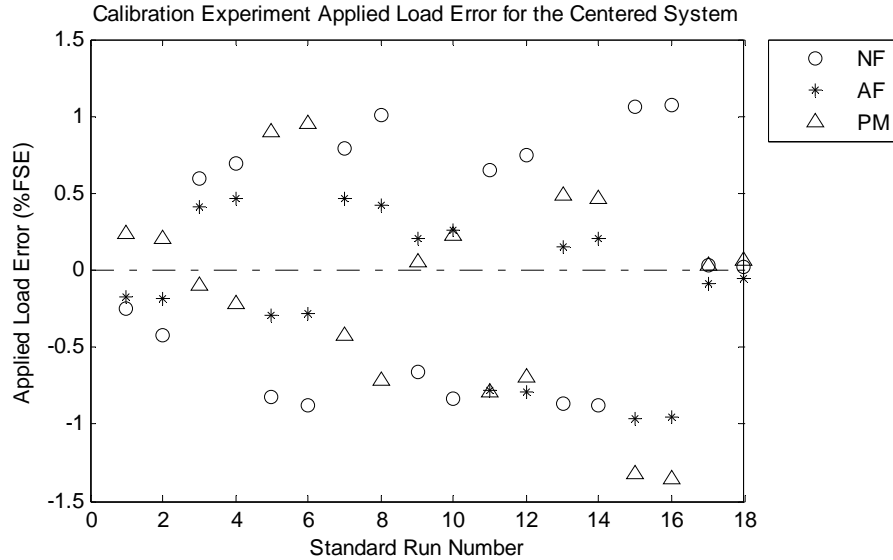


Figure 14. Applied Load Error for the Centered System Calibration Experiment

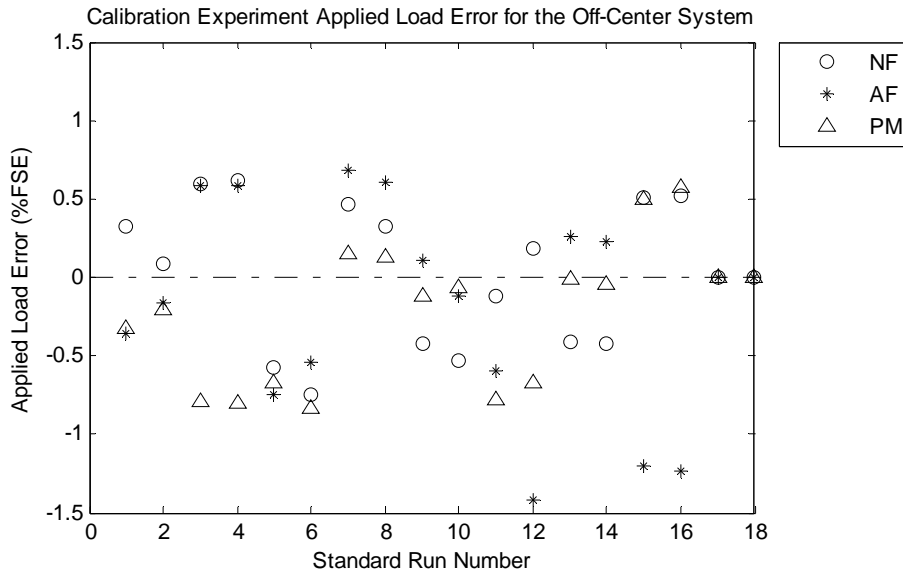


Figure 15. Applied Load Error for the Off-Center System Calibration Experiment

The summary statistics for the applied load errors are presented in table 11. While the 2σ errors are not to the level required for production balance calibrations, they are in a feasible range to consider further development of

this concept. The many factors contributing to the errors of this magnitude and potential areas to consider for improvement are:

- A more up to date calibration of the experimental balance
- Aerodynamic effects on the moving mass (a shrouded concept would be considered)
- Unaccounted for deflection of the balance relative to the location of the accelerometers
- Improved precision of the dimensional inspections (simple measurement techniques were utilized)
- Improved precision of accelerometers, the addition of precision rate gyros

Table 11. Statistical Summary of Calibration Experiments Applied Load Error

| | Centered System | | | Off-Center System | | |
|------------------|-----------------|----------|----------|-------------------|----------|----------|
| | E_{NF} | E_{AF} | E_{PM} | E_{NF} | E_{AF} | E_{PM} |
| Mean (%FSE) | 0.06 | -0.16 | -0.11 | 0.02 | -0.18 | -0.22 |
| 2σ (%FSE) | 1.34 | 0.98 | 1.40 | 0.75 | 1.33 | 0.84 |

Tables 12 and 13 show the current system capabilities and the projected capabilities if current state of the art components were employed to develop a production calibration system respectively. Additionally, propagating the uncertainties for the proposed system to applied loads results in the estimated uncertainties in table 14.

Table 12. Proof of Concept Independent Variable Uncertainties (Estimated)

| Variable | Uncertainty | Units |
|--------------|-------------|-------|
| u_{ω} | 0.001 | rev/s |
| u_R | 0.01 | in |
| u_D | 0.01 | in |
| u_{T_x} | 0.01 | in |
| u_L | 0.01 | in |
| u_{θ} | 0.08 | deg |
| u_{ϕ} | 0.05 | deg |
| u_{α} | 0.001 | deg |
| u_m | 0.001 | lbs |

Table 13. Proposed Independent Variable Uncertainties (Estimated)

| Variable | Uncertainty | Units |
|--------------|-------------|-------|
| u_{ω} | 0.0001 | rev/s |
| u_R | 0.0001 | in |
| u_D | 0.0001 | in |
| u_{T_x} | 0.0001 | in |
| u_L | 0.0001 | in |
| u_{θ} | 0.0040 | deg |
| u_{ϕ} | 0.0040 | deg |
| u_{α} | 0.0005 | deg |
| u_m | 0.0005 | lbs |

Table 14. Estimated Applied Load Uncertainty - Proposed System

| | NF (%FSE) | AF (%FSE) | PM (%FSE) |
|-------------------|-----------|-----------|-----------|
| Centered System | 0.034 | 0.022 | 0.050 |
| Off-Center System | 0.028 | 0.031 | 0.030 |

VI. Conclusion

The VACS concept was developed and presented as a new methodology for calibrating balances. One aspect of the VACS is a method wherein the mass utilized for calibration is held constant, and the acceleration is changed to thereby generate relatively large forces with relatively small test masses. Multiple forces can be applied to a force balance without changing the test mass, and dynamic forces can be applied by rotation or oscillating acceleration. If rotational motion is utilized, a mass is rigidly attached to a force balance, and the mass is exposed to a rotational field. A large force can be applied by utilizing a large rotational velocity. A centrifuge or rotating table can be used to create the rotational field, and fixtures can be utilized to position the force balance. The acceleration may also be linear. For example, a table that moves linearly and accelerates in a sinusoidal manner may also be utilized. The test mass does not have to move in a path that is parallel to the ground, and no re-leveling is therefore required. Balance deflection corrections may be applied passively by monitoring the orientation of the force balance with a three-axis accelerometer package. Deflections are measured during each test run, and adjustments with respect to the true applied load can be made during the post-processing stage.

The proof of concept systems, centered and off-center, were demonstrated and the calibration results provide data on the feasibility of the concept. Improvements required to bring the system into the level of capability necessary for production calibrations were shown. Additionally, some of the unique aspects of the concept were discussed.

Additional advantages of the concept include that the footprint of the VACS is small compared to any other calibration system currently in use. This could allow for the VACS to fit in a small bus or van to be used for rapid turnover, in-situ calibrations. The mobile system could travel to the wind tunnel of interest and perform a transducer calibration within a couple hours. Alternatively, the small footprint of the VACS could allow for the system to be placed in a temperature controlled chamber to allow for transducer calibration at multiple temperature levels.

Another feature unique to the VACS is that it is capable of calibrating multiple transducers simultaneously. With a sufficiently large rotating platform, up to eight transducers could feasibly be calibrated at once as shown in figure 16. This could allow for recalibration of NASA's inventory of force transducers, providing a vast improvement to operational readiness.

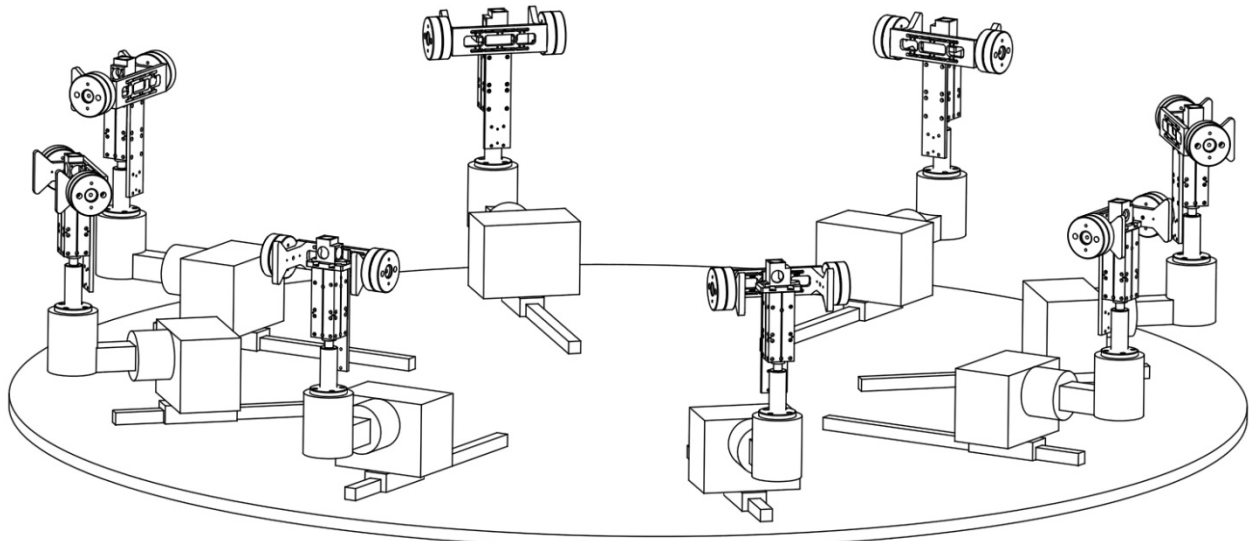


Figure 16. Multiple Balance Calibration Concept

Acknowledgments

Special thanks to Greg Jones, Chris Lynn, Mark Roth, Jeff Werner and Tom Finley for their support of this research.

References

¹Parker, P.A., Liu, T., "Uncertainty Analysis of the Single-Vector Force Balance Calibration System," AIAA-2002-2792, 22nd AIAA Aerodynamic Measurement Technology and Ground Testing Conference, St. Louis, Missouri, June 24-26, 2002.

²Parker, P.A., Morton, M., Draper, N., Line, W., "A Single-Vector Force Calibration Method Featuring the Modern Design of Experiments," AIAA 2001-0170, 39th Aerospace Sciences Meeting and Exhibit, Reno, Nevada, January 2001.

³Montgomery, D.C., *Design and Analysis of Experiments*, 6th ed., John Wiley & Sons, New York, 2005.

Filename: lf99-17936_final-Rhew_9th_ISSGB_v2
Directory: C:\Users\wbaize\AppData\Local\Temp\1
Template: C:\Users\lawrenceg\Desktop\Ann Ames request - 12-9-
13\Papers_Template_25Nov2013.dot
Title: Preparation of Papers for AIAA Technical Conferences
Subject:
Author: lawrenceg
Keywords:
Comments:
Creation Date: 4/14/2014 12:03:00 PM
Change Number: 9
Last Saved On: 4/14/2014 5:55:00 PM
Last Saved By: Ray Rhew
Total Editing Time: 13 Minutes
Last Printed On: 5/30/2014 11:20:00 AM
As of Last Complete Printing
Number of Pages: 19
Number of Words: 5,636 (approx.)
Number of Characters: 32,128 (approx.)